Available online at www.sciencedirect.com
ScienceDirect
Thermochimica Acta 463 (2007) 15–17
thermochimica acta
www.elsevier.com/locate/tca

Subsolidus binary phase diagram of $C_{12}Mn$–$C_{16}Mn$ in thermotropic phase transitions materials

Kezhong Wu [a,*], Weizhen Cui [b], Jianjun Zhang [a]

[a] *Department of Chemistry and Material Science, Hebei Normal University, Shijiazhuang 050016, China*
[b] *Department of Chemistry, Cangzhou Teachers College, Hebei Cangzhou 061001, China*

Available online 30 March 2007

Abstract

(n-$C_{12}H_{25}NH_3)_2MnCl_4$ and (n-$C_{16}H_{33}NH_3)_2MnCl_4$ were synthesized and a series of their mixtures $C_{12}Mn$–$C_{16}Mn$ prepared. The binary phase diagram of $C_{12}Mn$–$C_{16}Mn$ mixtures was established by differential thermal analysis (DTA) and X-ray diffraction (XRD). A new material of (n-$C_{12}H_{25}NH_3$)(n-$C_{16}H_{33}NH_3$)$MnCl_4$ and two eutectoid invariants were observed, and the two eutectic point temperatures are about 317 and 304 K. In comparison with other similar system, there are three noticeable solid solution ranges (α, β, γ) at the left boundary, right boundary, and middle of the phase diagram, respectively.

Keywords: Dodecylammonium tetrachloromanganate; Hexadecylammonium tetrachloromanganate; Phase diagram; DTA; XRD

1. Introduction

Compounds of the type A_2BX_4 or ABX_3 (A, B is metal; X is halogen or oxygen) have attracted considerable attention due to their physical properties, including ferro-, piezo- or pyroelectricity, ferri-, antiferro- or piezomagnetism and non-linear optical effects, and their technical applications for electro- or magneto-optical devices [1,2]. Similar physical and structural properties are observed when metal A is substituted by an $[NR_4]^+$ ion (R is H, alkyl, or aryl) [3–6]. Herein, we synthesized two materials of the type $[NR_4]_2MnCl_4$ in bis(n-alkylammonium) tetrachloromanganate(II) with the general formula (n-$C_{12}H_{25}NH_3)_2MnCl_4$ (short notation; $C_{12}Mn$) and (n-$C_{16}H_{33}NH_3)_2MnCl_4$ (short notation; $C_{16}Mn$). The two compounds are known to crystallize in a perovskite structure. The $MnCl_4^{2-}$ anions are sandwiched between double layers of n-alkylammonium cations. The layers are bound by van der Waals forces between $(CH_2)_nCH_3$ groups and by long-range Coulomb forces, and the tetrahedral cavities are occupied by the $-NH_3^+$ polar head of the n-alkylammonium cations which weak N–H···Cl hydrogen bonds with the halogens. The physical properties and structure of C_nMn [4–6] and C_nZn systems [7] have been previously researched. The binary phase diagram for $C_{10}Zn$–$C_{12}Zn$ [6], $C_{12}Zn$–$C_{18}Zn$ [8], $C_{10}Co$–$C_{16}Co$ [9] was reported. Among them, the diagram of $C_{10}Co$–$C_{16}Co$ compared with other shows absolute immiscibility. Now, the binary phase diagram of $C_{12}Mn$–$C_{16}Mn$ is not known. In this paper the subsolidus binary phase diagram of $C_{12}Mn$–$C_{16}Mn$ was established by differential thermal analysis (DTA) and X-ray diffraction (XRD).

2. Experimental procedure

$MnCl_2$, concentrated HCl and absolute ethanol were used as starting materials, which were of AR grade from Beijing Chemical Reagent Company. Dodecylamine (C.P.) was purchased from Tianjin Xiqing Kelong Reagent Plant (China). Hexadecylamine (A.P.) was purchased from ACROS ORGANICS (Germany).

$C_{12}Mn$ and $C_{16}Mn$ were prepared by the chemical method in Ref. [8] and analyzed with an MT-3 CHN elemental analyzer (Japan). The results of elemental analysis are in wt.%, Elemental analyses calc. (%) for $C_{12}Mn$: C 50.62, H 9.84, N 4.92; found: C 50.69, H 10.08, N 4.69. Anal. calc. (%) for $C_{16}Mn$: C 56.38, H 10.57, N 4.11; found: C 56.46, H 10.81, N 3.85. The $C_{12}Mn$ and $C_{16}Mn$ were weighed exactly in desired proportion to prepare different mixed samples. The two components were dissolved in absolute ethanol. Then part of the solvent was evaporated. Air-dry samples were put into a vacuum desiccator for 8 h at temperature about 253 K.

* Corresponding author. Tel.: +86 311 86268049.
E-mail address: wukzh688@163.com (K. Wu).

0040-6031/$ – see front matter © 2007 Elsevier B.V. All rights reserved.
doi:10.1016/j.tca.2007.03.019

The thermal behavior of the samples was investigated with a CDR-1 differential scanning calorimeter (DSC; Shanghai Scale Instrument Plant) at a scanning rate of 5 K/min^{-1} in a static atmosphere. Samples weighing about 5 mg were sealed in aluminum crucibles.

X-ray diffraction patterns on compacted samples of the powders were taken by D/MAX-RA X-ray diffractometer (made in Japan) using Cu Kα radiation (Ni filter) at a scanning rate of 2 min^{-1}. Voltage/electric current is 40 kV/100 mA.

3. Experimental results

3.1. Thermal analysis

The results of DTA experiments obtained with "Shape factors method" [10] are listed in Table 1. All the materials C_nMn show solid–solid phase transition in the temperature range 298–350 K. These are always reproducible after heating and cooling cycles throughout the transition points. The data in Table 1 shows that the value of the transition temperature decreases with increasing $W_{C_{12}Mn}$% in the range from 0 to 30.46%. Then, the phase transition temperature first rises to from 30.46 to 46.96%. The first eutectoid temperature (about 317 K) appears in the $W_{C_{12}Mn}$% range of 21.84–35.71%. The second decrease was found from 46.96 to 81.03%. With $W_{C_{12}Zn}$% increasing gradually from 81.03%, the phase transition temperature rises again. The second eutectoid temperature at about 304 K was found in the $W_{C_{12}Mn}$% range of 71.48–87.20%. Table 1 reveals that the first eutectic temperature is not close to $W_{C_{12}Mn}$% = 0, nor does the second eutectic temperature end near $W_{C_{12}Mn}$% = 100%. The range of the first eutectic temperature does not end close to the beginning of the second eutectic temperature. It is clear that the values of phase transition temperature of the binary system $C_{12}Mn$–$C_{16}Mn$ in solid-solid phase transitions show a waving dependence on $W_{C_{12}Mn}$%. The reason be sure that there are not only an intermediate (n-$C_{12}H_{25}NH_3$)(n-$C_{16}H_{33}NH_3$)$MnCl_4$ (short notation; $C_{12}C_{16}Mn$) but also three solid solution ranges exist at the left, right boundary and middle of the phase diagram of $C_{12}Mn$–$C_{16}Mn$.

Table 1
Solid–solid transition temperatures of the $C_{12}Mn$–$C_{16}Mn$ system with measured increasing temperature

$W_{C_{12}Mn}$ (%)	T_{e1} (K)	T_{e2} (K)	T_{s1} (K)	T_{s2} (K)
0 ($C_{16}Mn$)				350
4.17			344	346
9.00			339	342
18.40			327	332
21.84	317			329
26.05	317			327
30.46	317			320
35.71	317			321
43.14			321	323
46.96			321	323
50.85			318	321
58.00			315	319
62.59			312	315
66.56			307	314
71.48		304		312
75.91		304		310
81.03		304		308
84.89		304		313
87.20		304		314
93.67			310	321
96.33			323	327
100 ($C_{12}Mn$)				331

Note: T_e, eutectoid invariant; T_{s1}, onset temperature; T_{s2}, finish temperature.

3.2. X-ray diffraction

Table 2 summarizes the d values of strong peaks with bigger relative intensity at room temperature for pure $C_{12}Mn$, $C_{16}Mn$ and their mixtures. We find that the d value of sample with $W_{C_{12}Mn}$% of 9.00% has the similar d value to the pure $C_{16}Mn$, indicating a single-phase region. In this concentration range, $C_{12}C_{16}Mn$ dissolves in $C_{12}Mn$ to form a solid solution α. Similarly, samples with $W_{C_{12}Mn}$% from 96.33% to pure $C_{12}Mn$ have homologous patterns, revealing that $C_{12}C_{16}Mn$ dissolves in $C_{12}Mn$ to form a solid solution β. In the same way, samples $W_{C_{12}Mn}$% from 46.96 to 58.00% have similar diffraction patterns, showing that $C_{12}Mn$ or $C_{16}Mn$ dissolved in $C_{12}C_{16}Mn$, forming a single-phase γ. Samples with $W_{C_{12}Mn}$% from 21.48 to 35.71% are in the two-phase region, and their patterns are the overlap of α and γ. The patterns in $W_{C_{12}Mn}$% range of 71.48–87.20% are the overlap of β and γ, and in the two-phase region. This above evidence that led us to strongly support the fact that the form of intermediate (n-$C_{12}H_{25}NH_3$)(n-$C_{16}H_{33}NH_3$)$MnCl_4$ and three solid solution in the phase diagram of $C_{12}Mn$–$C_{16}Mn$.

3.3. Establishment of phase diagram

The binary phase diagram of $C_{12}Mn$–$C_{16}Mn$ (Fig. 1) was obtained according to the temperature-composition relations from the above DTA and X-ray diffraction experiments. Fig. 1 indicates that an intermediate compound ($C_{12}H_{25}NH_3$)–($C_{16}H_{33}NH_3$)$MnCl_4$ is formed, due to a top temperature between two eutectoid invariants [11]. The low temperature perovskite-layer structure of $C_{12}Mn$, $C_{16}Mn$ and their binary system are organized by neutralizing $MnCl_4^{2-}$ with

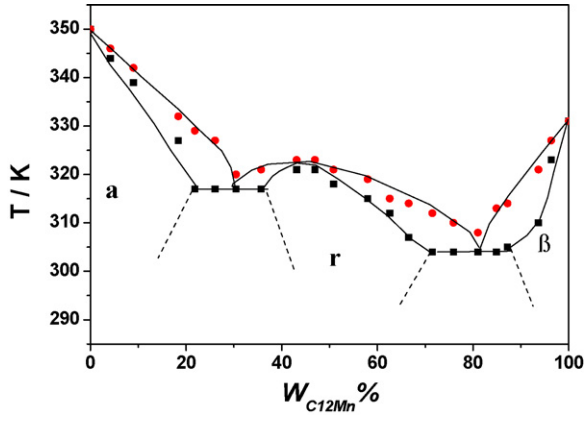

Fig. 1. Phase diagram of $C_{12}Mn$–$C_{16}Mn$ system.

Table 2
d (nm) values at room temperature

$C_{16}Mn$	9.00%	21.84%	26.05%	46.96%	58.00%	71.48%	87.20%	96.33%	$C_{12}Mn$
12.4051	12.3015	12.3704	12.3015	16.9803	16.8508	5.1630	5.1870	7.6485	7.4683
9.2630	9.2630	9.2824	9.2630	11.2387	11.1819	5.3049	5.0635	6.1036	6.0292
7.4059	7.3813	7.4557	7.3936	8.4342	8.4022	4.3624	4.3838	4.3582	4.2915
4.0920	4.0117	4.3838	4.3204	3.7048	3.7293	3.6957	3.7048	4.0117	3.9657
3.6866	3.6776	3.6957	3.6746	3.6274	3.6274	3.6245	3.6303	3.6927	3.7541
3.0681	3.0889	3.6129	3.6100	2.5844	2.5787	2.5801	2.5873	3.3858	3.3360
2.8787	2.8554	2.5744	2.5744			2.5474	2.5252	3.0415	3.0035
2.6270	2.6482							2.7659	2.7793
2.4940	2.4820							2.5573	2.5587
2.4518	2.4682							2.5335	2.5061
2.3098	2.3270							2.3422	2.3792
2.2985	2.2108							2.2467	2.2297

alkylammonium ions. Alkylammonium chains are parallel to each other and slightly tilted with respect to the normal of the inorganic layers. The adjacent alkyl chains interact with each other by van der Waals interaction, and are hydrogen bonded to $MnCl_4^{2-}$. When the temperature is increased to 317 K, the first eutectoid invariant occurs from 21.84 to 35.71%. $C_{12}Mn$ and $C_{12}C_{16}Mn$ undergo a reversible solid–solid phase transformation. In this situation, the chains are in a large degree of motional freedom and a disordered phase appears. At the same time, the hydrogen bonds are weakened and even destroyed. When the temperature is increased to 304 K, the second eutectoid invariant appears from 71.48 to 87.20%. Similarly, $C_{16}Mn$ and $C_{12}C_{16}Mn$ undergo a reversible solid-solid phase transformation.

A binary phase diagram for a homologous system of $C_{10}Co$–$C_{16}Co$ was reported [9], the shape of which is similar to ours. The largest difference is that their diagram shows absolute immiscibility, while partial miscibility was observed in this work. As is well known, the phase diagram of binary systems is determined by the difference of two components. If their structure and size of two components are little different, they often dissolve each other and form miscible system. Conversely, when they are much difference, the degree of miscibility is limited. $C_{12}C_{16}Mn$ was considered that $C_{12}Mn$ and $C_{16}Mn$ has exchanged a alkylammonium chains by each other, so their structure and molecular size have little difference, which results in their partial miscibility.

4. Conclusion

The binary phase diagram of $(n\text{-}C_{12}H_{25}NH_3)_2MnCl_4$ and $(n\text{-}C_{16}H_{33}NH_3)_2MnCl_4$ mixtures was established by DTA and XRD. A new material of $(n\text{-}C_{12}H_{25}NH_3)(n\text{-}C_{16}H_{33}NH_3)MnCl_4$ and two eutectoid invariants were observed. There are three noticeable solid solution ranges at the left boundary, right boundary, and middle of the phase diagram, respectively. The hydrogen bonds and van der Waals forces in the intermediate compound $(n\text{-}C_{12}H_{25}NH_3)(n\text{-}C_{16}H_{33}NH_3)MnCl_4$ and three solid solution ranges (α, β, γ) are stronger than that of other binary system, which are caused by the alkylammonium chains are an ordered phase in low degree of motional freedom. This results lead to the final transition temperature T_{s2} of the intermediate compound and the solid solution are higher than other binary system.

References

[1] J. Fenrych, E.C. Reynhardt, S. Jurga, et al., Mol. Phys. 78 (5) (1993) 1117–1128.
[2] R. Jakubas, M. Bator, M. Gosniowska, et al., J. Phys. Chem. Solids 58 (6) (1997) 989–998.
[3] N.V. Venkataraman, S. Barman, S. Vasudevan, et al., Chem. Phys. Lett. 358 (2002) 139–143.
[4] Y. Tabuchi, K. Asai, M. Rikukawa, et al., J. Phys. Chem. Solids 61 (2000) 837–845.
[5] K.Z. Wu, C.X. Zhang, Y.J. Li, et al., J. Chin. Chem. Soc. 52 (2005) 45–50.
[6] K.Z. Wu, P. Zuo, X.D. Liu, et al., Thermochim. Acta 397 (2003) 49–53.
[7] V. Busico, T. Tartaglione, M. Vacatello, Thermochim. Acta 62 (1983) 77–86.
[8] K.Z. Wu, X.D. Wang, X.D. Liu, J. Univ. Sci. Technol. Beijing 10 (4) (2003) 75–77.
[9] W.P. Li, D.S. Zhang, T.P. Zhang, et al., Thermochim. Acta 326 (1999) 183–186.
[10] R. Courchinoux, N.B. Chanh, Y. Haget, Thermochim. Acta 128 (1988) 45–53.
[11] P.W. Atkins, Physical Chemistry, Oxford University, Oxford, 1990.